Tunneling through an Anderson impurity between superconductors

Yshai Avishai,[1,*] Anatoly Golub,[1] and Andrei D. Zaikin[2,3]

[1]*Department of Physics, Ben-Gurion University of the Negev, Beer-Sheva, Israel*
[2]*Forschungszentrum Karlsruhe, Institut für Nanotechnologie, D-76021 Karlsruhe, Germany*
[3]*I.E. Tamm Department of Theoretical Physics, P.N. Lebedev Physics Institute, 117924 Moscow, Russia*

We consider an Anderson impurity (A) weakly connected to a superconducting electrode (S) on one side and a superconducting or a normal-metal electrode (N) on the other side. A general path-integral formalism is developed and the response of SAN and SAS junctions to a constant voltage bias V is elucidated, using a combination of the Keldysh technique (to handle nonequilibrium effects) and a dynamical mean-field approximation (to handle repulsive Hubbard interactions). An interesting physics is exposed at subgap voltages ($eV < \Delta$ for SAN and $eV < 2\Delta$ for SAS). For an SAN junction, Andreev reflection is strongly affected by Coulomb interaction. For superconductors with p-wave symmetry the junction conductance exhibits a remarkable peak at $eV < \Delta$, while for superconductors with s-wave symmetric pair potential the peak is shifted towards the gap edge $eV = \Delta$ and strongly suppressed if the Hubbard repulsive interaction increases. Electron transport in SAS junctions is determined by an interplay between multiple Andreev reflection (MAR) and Coulomb effects. For s-wave superconductors the usual peaks in the conductance that originate from MAR are shifted by interaction to larger values of V. They are also suppressed as the Hubbard interaction strength grows. For p-wave superconductors the subgap current is much larger and the I-V characteristics reveal an interesting feature, namely, a peak in the current resulting from a midgap bound state in the junction.

PACS number(s): 74.40.+k, 72.10.−d, 74.20.−z, 74.50.+r

I. INTRODUCTION

The dynamical behavior of Josephson junction strongly depends, among other factors, on its transparency. If the insulating barrier is not too high then the concept of nonlinear tunneling becomes relevant. In this case the characteristic dynamical conductance dI/dV at applied voltages V less than the superconducting gap Δ shows a subgap structure. An explanation of this behavior was given some time ago,[1,2] based on the mechanisms of multiple Andreev reflections (MAR). Recently, the subgap current was calculated for the case of electron tunneling through a junction with resonant impurity.[3] Rapid progress in the technology of superconducting junctions makes it possible to fabricate junctions composed of quantum dots weakly coupled to superconducting or normal electrodes. The basic physics of such a device can be elucidated once it is modeled as an Anderson impurity center. In this case the Coulomb interaction is expected to strongly affect the tunneling current in general and the subgap current in particular. Since the subgap current is originated from multiple Andreev reflections, its physics has a close similarity to that of the Josephson current. In this context, it is established[4] that the tunneling through a quantum dot is suppressed if the effective Kondo temperature $T_K = \sqrt{U\Gamma} \exp[-\pi|\epsilon_0|/2\Gamma]$ is small as compared with the superconducting gap Δ (hereafter, U is the Hubbard repulsion strength, ϵ_0 is the orbital energy of the dot electron, and Γ is the width of this energy state). Strong interaction-induced suppression of the current through superconducting quantum dots was also observed experimentally.[5]

Quite recently detailed measurements of I-V curves in atomic-size metallic contacts were performed.[6] An explanation of the observed I-V curves were given[7] in terms of the atomic valence orbitals which represent different conducting channels. The Coulomb interaction was considered there to be screened as in bulk metals. However, for quantum dots and break junctions the screening is virtually ineffective and an unscreened Hubbard-type repulsive interaction emerges. In this case the Kondo temperature T_K becomes a relevant parameter, separating levels with $T_K > \Delta$ (which are responsible for high, nearly resonant conductance) from levels with $T_K < \Delta$, in which the conductance is strongly influenced by interaction.

In recent experiments, a tunable Kondo effect in semiconducting quantum dot devices[8,9] was investigated. It was clearly demonstrated there that tunneling through a single level (out of numerous levels formed by electron confinement in the dot) takes place. In such dots, the interaction of electrons U strongly influences the bare orbital energy ϵ_0. In the case of quantum dots with superconducting leads we then expect the superconducting gap at the leads and the connection of the dot to the leads to play an important role for both SAS and SAN junctions. Depending on relative values of theses parameters different regimes for the tunneling current are possible. One is the Kondo regime considered in Refs. 10–12.

In the present paper we study the other regime when the impurity is singly occupied, and develop a detailed theoretical analysis of an interplay between the phenomena of MAR and Coulomb interaction in quantum dots with superconducting leads. Both MAR and Coulomb effects have been intensively studied in the literature over the past decades; here we elucidate an interplay between them. When combined together in quantum dots, these two phenomena, lead to interesting physical effects and — depending on parameters — may dramatically influence the subgap conductance pattern of the system. Another important issue in the study of SAS and SAN junctions is the parity of the order parameter of the

63 134515-1

superconducting electrodes. For example, the order parameter of the recently discovered[13] superconducting material Sr_2RuO_4 is believed to have a p-wave symmetry.[14] If a superconductor of this type is properly oriented with respect to the tunneling direction the principal contribution to the Josephson current comes from a bound state[16,17] formed at the contact point. This bound state arises since the pair potential has an opposite sign for injected and reflected quasiparticles and is expected to play an important role in the formation of subgap currents.

The rich physics of SAS and SAN junctions subject to a finite potential bias is exposed below. In particular, we calculate the tunneling current and the dynamical conductance for junctions consisting of s- and p-wave superconductors. The main steps required for treating the pertinent many-body problem can be summarized as follows: (i) Taking the Fermi energy of the unbiased lead as an energy reference, the site energy ϵ_0 of the Anderson impurity is chosen such that $\epsilon_0 < 0$ while $U + \epsilon_0 > 0$. These inequalities assure that assuming the quantum dot to be at most singly occupied should be an excellent approximation. (ii) To handle the strong interaction appearing in the Hubbard term, a mean-field approximation[18,19] is adopted. (iii) The formalism should take into account the nonequilibrium nature of the physical system. For this purpose, the standard approach is to start from the expression for the kernel of the evolution operator or the generating functional, which is the analog of the partition function in the equilibrium case, evaluated, however, on a Keldysh contour[20] (see review article in Ref. 21). At the end of this procedure one is able to calculate the SAN Andreev conductance analytically, and to get expressions for the nonlinear response of SAS junctions which are amenable for numerical evaluation.

The technical procedure by which we manage to advance the calculations is detailed below in Sec. II, where we derive an effective action for SAS and SAN junctions. In Sec. III we discuss the dynamical mean-field approximation adopted in the present work in order to treat interaction effects. Concrete results pertaining to subgap current in SAS junctions and differential conductance in SAN junctions are presented and discussed in Sec. IV. The paper is then concluded and summarized in Sec. V. Some technical details of the calculation are given in the Appendix.

II. GENERAL ANALYSIS

A. Model

Consider a system consisting of two superconducting wide strips on the left ($x < 0, -\infty < y < \infty$) and on the right ($x > 0, -\infty < y < \infty$) weakly connected by a quantum dot through which an electron tunneling takes place. This system can be described by the Hamiltonian

$$H = H_L + H_R + H_{\text{dot}} + H_t. \tag{1}$$

The Hamiltonians of the left and right superconducting electrodes have the standard BCS form,

$$H_j = \int dr [\Psi_{j\sigma}^\dagger(r) \xi(\nabla) \Psi_{j\sigma}(r)$$
$$- \lambda \Psi_{j\uparrow}^\dagger(r) \Psi_{j\downarrow}^\dagger(r) \Psi_{j\downarrow}(r) \Psi_{j\uparrow}(r)]. \tag{2}$$

Here $\Psi_{j\sigma}^\dagger$ ($\Psi_{j\sigma}$) are the electron creation (annihilation) operators, λ is the BCS coupling constant, $\xi(\nabla) = -\nabla^2/2m - \mu$, and $j = L, R$. Here and below we set the Planck's constant $\hbar = 1$. Whenever appropriate, the spin, space, and time dependence of all the field operators will not be explicitly displayed.

The quantum dot is treated as an Anderson impurity center located at $x = y = 0$. It is described by the Hamiltonian

$$H_{\text{dot}} = \epsilon_0 \sum_\sigma C_\sigma^\dagger C_\sigma + U C_\uparrow^\dagger C_\uparrow C_\downarrow^\dagger C_\downarrow, \tag{3}$$

where $C_\sigma^\dagger$ and C_σ are the electron operators in the dot. The impurity site energy ϵ_0 (counted from the Fermi energy μ) is assumed to be far below the Fermi level (that is, $\epsilon_F = 0$, $\epsilon_0 \ll 0$. The presence of a strong Coulomb repulsion $U > -\epsilon_0$ between electrons in the same orbital guarantees that the dot is at most singly occupied.

Electron tunneling through the dot is accounted for by means of the term

$$H_t = \sum_{j=L,R} \mathcal{T}_j \sum_\sigma \Psi_{j\sigma}^\dagger(0) C_\sigma + \text{H.c.}, \tag{4}$$

where $\mathcal{T}_{L(R)}$ are the effective transfer amplitudes between the left (right) electrode and the dot.

In what follows we will always assume that, if a bias voltage V is applied to the system from, say, right to left, the entire voltage drop occurs across the dot. Hence the quasiparticle distribution functions in the leads are the Fermi ones, with the chemical potentials of the electrodes shifted with respect to each other by eV.

B. Evolution operator

Complete information about the quantum dynamics of the system is contained within the evolution operator defined on the Keldysh contour[20] K (which consists of forward and backward oriented time branches). The kernel J of this evolution operator can be expressed in terms of a path integral,

$$J = \int \mathcal{D}\bar{\Psi} \mathcal{D}\Psi \mathcal{D}\bar{C} \mathcal{D}C \exp(iS), \tag{5}$$

over the fermion fields corresponding to the operators $\Psi^\dagger$, Ψ, $C^\dagger$, and C [here the field $\bar{\Psi}$ corresponds to ($\Psi_{L\uparrow}^\dagger, \Psi_{L\downarrow}^\dagger, \Psi_{R\uparrow}^\dagger, \Psi_{R\downarrow}^\dagger$) and similarly for other fields], $S = \int_K L dt$ is the action and L is the Lagrangian pertaining to the Hamiltonian (1). The external fields (e.g., electromagnetic fields) can be treated as the source terms for the action, though the fluctuating parts of these fields should be integrated as well.

Usually it is convenient to perform an operator rotation $C \rightarrow c$ and $\Psi \rightarrow \psi$ in Keldysh space:

$$\bar{c}=\bar{C}\hat{Q}^{-1}, \quad c=\hat{Q}\sigma_z C; \quad \bar{\psi}=\bar{\Psi}\hat{Q}^{-1}, \quad \psi=\hat{Q}\sigma_z\Psi. \quad (6)$$

Here σ_z is one of the Pauli matrices σ_x, σ_y, σ_z operating in the Keldysh space and

$$\hat{Q}=\frac{1}{\sqrt{2}}\begin{pmatrix} 1 & -1 \\ 1 & 1 \end{pmatrix} \quad (7)$$

is the Keldysh matrix. The Grassman variables $\bar{c}$, c, $\bar{\psi}$, ψ are now defined solely on the forward time branch.

The transformation of the Green functions follows directly from Eq. (6). One starts from the 2×2 matrix $\hat{\bar{G}}$ of the Green functions defined in terms of the initial electron operators. The elements of the matrix $\hat{\bar{G}}$ are the Green functions $\hat{\bar{G}}_{ij}$ with $i,j=+,-$ according to whether the time belongs to the upper or the lower branch of the Keldysh contour K. Of these four Green functions only three are independent. Under the operator rotation (6) the Green-Keldysh matrix $\hat{\bar{G}}$ is transformed as $\hat{G}=Q^{-1}\hat{\bar{G}}Q$, where

$$\hat{G}=\begin{pmatrix} \hat{G}^R & \hat{G}^K \\ \hat{0} & \hat{G}^A \end{pmatrix} \quad (8)$$

and

$$\hat{G}^R=-i\theta(t-t')\langle\psi(r,t)\psi^\dagger(r',t')+\psi^\dagger(r',t')\psi(r,t)\rangle,$$

$$G^A=i\theta(t'-t)\langle\psi(r,t)\psi^\dagger(r',t')+\psi^\dagger(r',t')\psi(r,t)\rangle,$$

$$G^K=-i\langle\psi(r,t)\psi^\dagger(r',t')-\psi^\dagger(r',t')\psi(r,t)\rangle, \quad (9)$$

are respectively retarded, advanced and Keldysh Green functions. Each of these matrices is in turn 2×2 matrix in the Nambu space.

The path integral (5) is now expressed in terms of the new Grassman variables

$$J=\int \mathcal{D}\bar{\psi}\mathcal{D}\psi\mathcal{D}\bar{c}\mathcal{D}c \exp(iS_{\text{dot}}+iS_0[\bar{\psi},\psi]), \quad (10)$$

where

$$S_{\text{dot}}=\int dt\left[\bar{c}\left(i\frac{\partial}{\partial t}-\tilde{\epsilon}\tau_z\right)c+\frac{U}{2}(\bar{c}c)^2\right], \quad (11)$$

$$S_0=\int dt\sum_{j=L,R}\left[\int_j dr\bar{\psi}_j(r,t)\hat{G}_j^{-1}\psi_j(r,t)\right.$$

$$\left. +(\mathcal{T}\bar{\psi}_j(0,t)\tau_z c(t)+\text{c.c.})\right]. \quad (12)$$

Here we defined $\tilde{\epsilon}=\epsilon_0+U/2$. In order to obtain the expression for the operator $\hat{G}_j^{-1}$ we employ the standard Hubbard-Stratonovich transformation of the quartic term in Eq. (2) and introduce additional path integrals over the complex scalar order parameter field $\Delta(r,t)$ defined on the Keldysh contour, see, e.g., Ref. 21. Here we are not interested in the fluctuation effects for the order-parameter field, and the path

integral over Δ is then evaluated by means of the saddle-point approximation. Quantitatively, it amounts to setting $\Delta(r,t)$ equal to the equilibrium superconducting order parameter values $\Delta_{L,R}$ of the left and the right electrodes. If needed, fluctuations of the order parameter field (both the amplitude and the phase) can easily be included into our consideration along the same lines as it was done in Ref. 21. Disregarding such fluctuations here, we find

$$\hat{G}_{L,R}^{-1}(\xi)=i\frac{\partial}{\partial t}-\tau_z\xi(\nabla)+\tau_+\Delta_{L,R}+\tau_-\Delta_{L,R}^*, \quad (13)$$

where we define $\tau_\pm=(\tau_x\pm i\tau_y)/2$. Here and below τ_x,τ_y,τ_z is the set of Pauli matrices operating in the Nambu space (for the sake of clarity we chose a different notation from that used for Pauli matrices operating in the Keldysh space).

C. Effective action

Let us now proceed with the derivation of the effective action for our model. We first notice that the ψ-fields dependent part S_0 of the total action is quadratic in these fields. Hence the integrals over $\bar{\psi}$ and ψ in Eq. (10) can be evaluated exactly, resulting in an action $S_{\text{env}}(\bar{c},c)$, formally defined as

$$\exp(iS_{\text{env}}[\bar{c},c])=\int \mathcal{D}\bar{\psi}\mathcal{D}\psi \exp(iS_0[\bar{\psi},\psi]). \quad (14)$$

Its physical content can be understood as follows: One can say that electrons in the two superconducting bulks serve as an effective environment for the quantum dot. Integrating out these electron variables in the spirit of the Feynman-Vernon influence functional approach[22] one arrives at the "environment" contribution to the action S_{env} expressed only in terms of the Anderson impurity variables $\bar{c}$ and c.

Due to the fact that coupling to the leads is concentrated at one point $(x,y)=(0,0)$ we can integrate out the fields inside the superconductors (hereafter referred as bulk fields) and obtain an effective action in terms of fermion operators with arguments solely on the surface. In order to achieve this central goal let us first note that translation invariance along y permits the Fourier-transform in Eq. (12) in this direction. The problem then reduces to a one-dimensional one with fermion fields $\psi_k(x)$ where k is the momentum along y. Gaussian integration over the bulk fields can be done with the help of the saddle-point method.

Let us consider, say, the left superconductor and omit the subscript $j=L$ for the moment. The pertinent equation for the optimal field reads

$$\hat{G}^{-1}(\xi_x)\tilde{\psi}_k(x)=0, \quad (15)$$

where $\xi_x=-(1/2m)(\partial^2/\partial x^2)-\mu_k$ and $\mu_k=\mu-k^2/2m$.

Let us decompose $\tilde{\psi}_k(x)=\psi_k^b(x)+\psi_k(0)$ in such a way that on the surface one has $\psi_k^b(0)=0$. The bulk field $\psi_k^b(x)$ satisfies the inhomogeneous equation

$$\hat{G}^{-1}(\xi_x)\psi_k^b(x)=-\mu_k\tau_z\psi_k(0). \quad (16)$$

In the right-hand side of this equation we employed the standard quasiclassical (Andreev) approximation which makes use of the fact that the superconducting gap as well as other typical energies of the problem are all much smaller than the Fermi energy.

In order to solve Eq. (16) we find the Green function $\hat{G}_k(x,t;x',t')$ (which satisfies the same equation albeit with a δ function on the right-hand side) and require $\hat{G}$ to vanish at $x=0$. The solution of Eq. (16) is then exploited to express $\psi_k^b(x)$ in terms of the surface fields $\psi_k(0)$. Combining the result with Eq. (12) we arrive at the intermediate effective action $\tilde{S}$ for a superconducting electrode which depends on the ψ fields at the surface,

$$\tilde{S}=i\int dt\int dt'\sum_k \frac{v_x}{2}\bar{\psi}_k(0,t)\hat{g}(t,t')\tau_z\psi_k(0,t'), \quad (17)$$

where $v_x=\sqrt{2\mu_k/m}$ is the quasiparticle velocity in the x direction. For a uniform superconducting half space (here the left one), the Green-Keldysh matrix

$$\hat{g}(t,t')\tau_z=-i\frac{v_x}{2}\frac{\partial}{\partial x}\int_L dx'\hat{G}_k(x,t;x',t')|_{x=0} \quad (18)$$

[which has the structure (8)] is expressed in terms of the Eilenberger functions[23] as follows:

$$\hat{g}(t,t')=e^{i\varphi(t)\tau_z/2}\int \hat{g}(\epsilon)e^{-i\epsilon(t-t')}\frac{d\epsilon}{2\pi}e^{-i\varphi(t')\tau_z/2}, \quad (19)$$

where

$$\hat{g}^{R/A}(\epsilon)=\frac{(\epsilon\pm i0)\tau_z+i|\Delta|\tau_y}{\sqrt{(\epsilon\pm i0)^2-|\Delta|^2}}, \quad (20)$$

$$\hat{g}^K(\epsilon)=[\hat{g}^R(\epsilon)-\hat{g}^A(\epsilon)]\tanh(\epsilon/2T). \quad (21)$$

Here $\varphi(t)=\varphi_0+2e\int^t V(t_1)dt_1$ is the time-dependent phase of the superconducting order parameter and $V(t)$ is the electric potential of the superconducting electrode.

An identical procedure applies for the right electrode. Each superconductor is thus described by a zero-dimensional action, respectively $\tilde{S}_L$ and $\tilde{S}_R$, coupled by an on-site hopping term with the Anderson impurity. It is now possible to integrate out these surface fields. The integral

$$\tilde{J}=\int \mathcal{D}\bar{\psi}(0)\mathcal{D}\psi(0)$$

$$\times\exp\left\{i\tilde{S}_{L,R}+i\int dt[\mathcal{T}_{L,R}\bar{\psi}_k(0)\tau_z c+\text{c.c.}]\right\} \quad (22)$$

can easily be evaluated, so that the contribution of the superconductors to the total effective action of our model is manifested in S_{env} defined as

$$S_{\text{env}}=2i\int dt\int dt'\sum_k \bar{c}(t)\left(\frac{\mathcal{T}_L^2}{v_x}\hat{g}_L(t,t')\right.$$

$$\left.+\frac{\mathcal{T}_R^2}{v_x}\hat{g}_R(t,t')\right)\tau_z c(t'). \quad (23)$$

Note that in deriving Eq. (23) we made use of the normalization condition[23] $\hat{g}_{L,R}^2=1$.

Equation (23) is valid for an arbitrary pairing symmetry. In the case of unconventional superconductors the Green functions $\hat{g}_{L,R}$ depend explicitly on the direction of the Fermi velocity. For uniform s-wave superconductors such dependence is absent and Eq. (23) can be simplified further. Defining the tunneling rates between the left (right) superconductor and the dot as

$$\Gamma_{L(R)}=4\sum_k \frac{\mathcal{T}_{L(R)}^2}{v_x}, \quad (24)$$

we obtain

$$S_{\text{env}}=\frac{i}{2}\int dt\int dt'\bar{c}(t)[\Gamma_L\hat{g}_L(t,t')+\Gamma_R\hat{g}_R(t,t')]\tau_z c(t'). \quad (25)$$

Concerning the definition (24) some comment is in order. The focus of attention here is the case in which there is a single conducting channel in the dot. In this situation, the transfer amplitudes $\mathcal{T}_{L,R}$ should effectively differ from zero only for $|v_x|\approx v_F$. One can easily generalize the action (25) to the situation with several or even many conducting channels. In this case the summation over momentum (essentially equivalent to the summation over conducting modes) should be done in Eq. (25) and some other dependence of $\mathcal{T}_{L,R}^2$ on v_x should apply. For instance, for tunnel junctions in the many channel limit one can demonstrate that[24] $\mathcal{T}_{L,R}^2\propto v_x^3$. It is also quite clear that the transfer amplitudes $\mathcal{T}_{L,R}$ *cannot* be considered as constants independent of the Fermi velocity direction, as it is sometimes assumed in the literature. In that case the sum (24) would simply diverge at small v_x in a clear contradiction with the fact that quasiparticles with $v_x\to 0$ should not contribute to the current at all. This ''paradox'' is resolved in a trivial way: the amplitudes $\mathcal{T}_{L,R}$ do depend on v_x and, moreover, they should vanish at $v_x\to 0$. For further discussion of this point we refer the reader to Ref. 24.

Combining Eqs. (10) and (14) we arrive at the expression for the kernel of the evolution operator J solely in terms of the fields $\bar{c}$ and c:

$$J=\int \mathcal{D}\bar{c}\mathcal{D}c\exp(iS_{\text{eff}}), \quad S_{\text{eff}}[\bar{c},c]=S_{\text{dot}}+S_{\text{env}}. \quad (26)$$

Here $S_{\text{eff}}[\bar{c},c]$ [defined by Eqs. (11) and (25)] represents the effective action for a quantum dot between two superconductors.

D. Transport current

In order to complete our general analysis let us express the current through the dot in terms of the correlation function for the variables $\bar{c}$ and c. This goal can be achieved by various means. For instance, one can treat the superconducting phase difference across the dot as a source field in the effective action and obtain the expression for the current just by varying the corresponding generating functional with respect to this phase difference. Another possible procedure is to directly employ the general expression for the current in terms of the Green-Keldysh functions of one (e.g., the left) superconductor, with arguments at the impurity site:

$$I = \frac{e}{4m} \int dy (\partial_x - \partial_{x'}) \text{Tr}[\hat{G}^K(xy, x'y'; t)]_{x=x'}, \quad (27)$$

where the trace is taken in Nambu space.

As before, it is convenient to separate the computation in terms of bulk and surface variables. After a simple algebra we transform Eq. (27) into the following result:

$$I = -i\frac{e}{4} \sum_k v_x \text{Tr}[\hat{g}_L \hat{G}_\psi - \text{H.c.}]|_K, \quad (28)$$

where $G_\psi = -i\langle \psi_k(0) \bar{\psi}_k(0) \rangle$ is the Green-Keldysh function for the surface ψ fields. Here and below the integration over the internal time variables in the product of matrices is implied and $(\cdots)|_K$ means the Keldysh component of this product.

Finally, let us express the function $\hat{G}_\psi$ in terms of the correlator for the fields $\bar{c}$ and c. Consider the generating functional for the surface fields

$$Z[\bar{\eta}, \eta] = \tilde{J}[\mathcal{T}_L \bar{\tau}_z c + \bar{\eta}, \mathcal{T}_L \tau_z c + \eta], \quad (29)$$

where the path integral $\tilde{J}$ is defined in Eq. (22). The functional derivative of Eq. (29) with respect to the η fields just yields the function $\hat{G}_\psi$:

$$\hat{G}_\psi = i\frac{\delta^2 Z}{\delta\bar{\eta}\delta\eta}\Big|_{\bar{\eta}=\eta=0}. \quad (30)$$

Evaluating the path integral (29) and making use of Eq. (30) we arrive at the following identity:

$$i\hat{G}_\psi = -\frac{2}{v_x}\hat{g}_L\tau_z + \frac{4\mathcal{T}_L^2}{v_x^2}\langle c\bar{c}\rangle. \quad (31)$$

Combining Eqs. (28) and (31) with the condition $\hat{g}_L^2 = 1$ we observe that the contribution of the first term in the right-hand side of Eq. (31) to the current vanishes identically, and only the second term $\propto \langle c\bar{c}\rangle$ turns out to be important. Making use of the definition (24) and symmetrizing the final result with respect to R and L we arrive at the following expression for the current:

$$I = \frac{e}{8}\text{Tr}[(\Gamma_L \hat{g}_L - \Gamma_R \hat{g}_R)\langle \bar{c}c\rangle|_K + \text{H.c.}]. \quad (32)$$

This expression completes our task. We have demonstrated that in order to calculate the current through an interacting quantum dot between two superconducting electrodes it is sufficient to evaluate the correlator $\langle \bar{c}c\rangle$ in the model defined by the effective action $S_{\text{eff}} = S_{\text{dot}} + S_{\text{env}}$ [Eqs. (11) and (25)]. Our approach enables one to investigate both equilibrium and nonequilibrium electron transport in superconducting quantum dots. In the noninteracting limit $U \to 0$ the problem reduces to a Gaussian one. In this case it can easily be solved and, as we will demonstrate below, the well known results describing normal and superconducting contacts without interaction can be recovered in a straightforward manner. In the interacting case $U \neq 0$ the solution of the problem naturally involves certain approximations. One of them, the dynamical mean-field approximation, is described in the next section.

III. MEAN-FIELD APPROXIMATION

In order to proceed further let us decouple the interacting term in Eq. (11) by means of a Hubbard-Stratonovich transformation[18,19] introducing additional scalar fields $\gamma_\pm$. The kernel J now reads

$$J = \int \mathcal{D}\bar{c}\mathcal{D}c\mathcal{D}\gamma_+\mathcal{D}\gamma_- \exp\left[iS[\gamma] + i\int dt\bar{c}\left(i\frac{\partial}{\partial t} - \tilde{\epsilon}\tau_z\right)c\right], \quad (33)$$

$$S[\gamma] = \int dt\left(\bar{c}\gamma_+\sigma_x c + \bar{c}\gamma_- c - \frac{2}{U}\gamma_+\gamma_-\right). \quad (34)$$

These equations are still exact. Now let us assume that the effective Kondo temperature $T_K = \sqrt{U\Gamma}\exp[-\pi|\epsilon_0|/2\Gamma]$ is smaller than the superconducting gap Δ. In this case, interactions can be accounted for within the dynamical mean-field (MF) approximation (see *SAN* section for more details). Notice that in equilibrium, an elaborate approximation was suggested recently in Ref. 25. The fields $\gamma_\pm$ in Eq. (34) can be determined from the saddle-point conditions

$$\delta J/\delta\gamma_\pm = 0. \quad (35)$$

In general these two equations contain an explicit dependence on the time variable. Let us average these equations over time and consider $\gamma_\pm$ as time independent parameters. This approximation is equivalent to retaining only the first moment of $\gamma_\pm$. The self-consistency Eqs. (35) now read

$$\gamma_+ = \frac{U}{2}\int dt\langle \bar{c}c\rangle, \quad (36)$$

$$\gamma_- = \frac{U}{2}\int dt\langle \bar{c}\sigma_x c\rangle. \quad (37)$$

As it turns out from our numerical analysis (to be described below), the parameter γ_+ has a negligible effect on the sub-gap current. It just slightly renormalizes the coupling constants $\mathcal{T}_{L,R}$ of our model. On the other hand, the second parameter, γ_-, which has (see below) the physical meaning as an energy proportional to the difference of spin up and down

populations of electrons on the level, strongly influences the *I-V* characteristics. Therefore in what follows we will set $\gamma_+ = 0$ and take into account only the second self-consistency Eq. (37) for γ_-. Under this approximation the effective action of our model acquires the following form:

$$S_{\text{eff}}[\gamma] = \int \frac{d\epsilon}{2\pi} \int d\epsilon' \bar{c} \hat{M}(\epsilon, \epsilon') c, \qquad (38)$$

$$\hat{M}(\epsilon, \epsilon') = \delta(\epsilon - \epsilon')[\epsilon + \gamma_- - \tau_z \tilde{\epsilon} + i(\Gamma_R/2)\hat{g}_R(\epsilon)\tau_z]$$
$$+ i(\Gamma_L/2)\hat{g}_L(\epsilon, \epsilon')\tau_z. \qquad (39)$$

Here and below we deliberately choose the electrostatic potential of the right electrode to be equal to zero, for which case the Keldysh matrix $\hat{g}_R$ is diagonal in energy space. Performing the functional integration over Grassman variables $\bar{c}$ and c we can cast the self-consistency Eq. (37) for γ_- in terms of the matrix

$$\hat{M}^{-1} = \begin{pmatrix} (\hat{M}^R)^{-1} & -(\hat{M}^R)^{-1}\hat{M}^K(\hat{M}^A)^{-1} \\ \hat{0} & (\hat{M}^A)^{-1} \end{pmatrix}, \qquad (40)$$

where $\hat{M}^R$, $\hat{M}^A$, $\hat{M}^K$ are three independent elements of the Keldysh matrix $\hat{M}$ (39). Recall that each of these elements is a 2×2 matrix in the Nambu space and an infinite matrix in the energy space. Equation (37) for γ_- can now be rewritten as

$$\gamma_- = i\frac{U}{2}\text{Tr}(\hat{M}^R)^{-1}\hat{M}^K(\hat{M}^A)^{-1}, \qquad (41)$$

with the trace being taken both in energy and spin spaces.

Finally, employing the MF approximation for the Hubbard interaction as was implied in the calculation of γ_-, we get the current as a difference of symmetric forms,

$$I = \frac{e\Gamma_L\Gamma_R}{8}\text{Tr}[(\hat{N}_L\hat{g}_R^R - (L \leftrightarrow R)) + \text{H.c.}], \qquad (42)$$

$$\hat{N}_{L,R} = (\hat{M}^R)^{-1}\hat{g}_{L,R}^K\tau_z(\hat{M}^A)^{-1}.$$

Consider now the case of a constant (time-independent) voltage bias V and recall that the entire voltage drop occurs across the quantum dot. Setting the phase of the right electrode equal to zero, we obtain, for the phase of the left superconductor, $\varphi(t) = 2eVt + \varphi_0$. Let us express $\hat{g}_L$ in terms of the matrix elements in energy space[2]

$$(\epsilon|\hat{g}_L|\epsilon') = \sum_{s=0,\pm 1} \delta(\epsilon - \epsilon' + 2seV)\hat{g}_L(\epsilon, \epsilon + 2seV), \qquad (43)$$

$$\hat{g}_L(\epsilon, \epsilon + 2seV) = [\hat{g}_L^{11}(E - eV)P_+ + g_L^{22}(\epsilon + eV)P_-]\delta_{0,s}$$
$$+ e^{i\varphi_0}g_L^{12}(\epsilon - eV)\tau_+\delta_{s,-1} + e^{-i\varphi_0}g_L^{21}$$
$$\times (\epsilon + eV)\tau_-\delta_{s,1}, \qquad (44)$$

where the superscripts denote the matrix elements in Nambu space and $P_\pm = (1 \pm \tau_z)/2$.

In what follows we shall abbreviate $\hat{g}_L(\epsilon + 2meV, \epsilon + 2neV) = (m|\hat{g}_L(\epsilon)|n)$ where the right-hand side is obtained from Eq. (44) after replacing $\epsilon \to \epsilon + 2meV$, $\delta_{0,s} \to \delta_{m,n}$, $\delta_{-1,s} \to \delta_{n,m-1}$, and $\delta_{1,s} \to \delta_{n,m+1}$. Then we have

$$\hat{g}_L(\epsilon, \epsilon') = \sum_n \delta(\epsilon - \epsilon' + 2neV)(0|\hat{g}_L(\epsilon)|n). \qquad (45)$$

The matrix M (39) may also be represented in a similar form, that is,

$$\hat{M}(\epsilon, \epsilon') = \sum_n \delta(\epsilon - \epsilon' + n2eV)[0|\hat{M}(\epsilon)|n], \qquad (46)$$

where

$$[m|\hat{M}(\epsilon)|n] = \delta_{m,n}\left[\epsilon + m2eV + \gamma_- - \tau_z\tilde{\epsilon}\right.$$
$$+ \frac{i\Gamma_R}{2}\hat{g}_R(\epsilon + m2eV)\tau_z\bigg]$$
$$+ \frac{i\Gamma_L}{2}[m|\hat{g}_L(\epsilon)|n]\tau_z. \qquad (47)$$

The integration over energy variables in the self-consistent equation for γ_- and in the expression for the time averaged current is conveniently performed by dividing the whole energy domain into slices of width $2eV$ and performing energy integration on an interval $[0 < E < 2eV]$. Thus we can use the discrete representation (47) and write

$$\gamma_- = i\frac{U}{2}\int_0^{2eV}\frac{d\epsilon}{2\pi}\sum_n \text{Tr}[n|(\hat{M}^R)^{-1}\hat{M}^K(\hat{M}^A)^{-1}|n], \qquad (48)$$

$$I = \frac{e\Gamma_L\Gamma_R}{8}\int_0^{2eV}\frac{d\epsilon}{2\pi}\sum_n \text{Tr}(n|[(\hat{N}_L\hat{g}_R^R - (L \leftrightarrow R)) + \text{H.c.}]|n). \qquad (49)$$

Let us also note that in the case of *SAN* junctions the expressions for the current and for γ_- can be further simplified. In this case Eq. (42) takes the form

$$I = \frac{e\Gamma_L\Gamma_R}{2}\int_{-\infty}^{\infty}\frac{d\epsilon}{2\pi}\text{Tr}(\{[\hat{M}^R(\epsilon)]^{-1}\hat{f}(\epsilon, V)[\hat{M}^A(\epsilon)]^{-1}\hat{g}_R^A(\epsilon)$$
$$- [\hat{M}^R(\epsilon)]^{-1}\hat{f}(\epsilon, 0)\hat{g}_R^A(\epsilon)\tau_z[\hat{M}^A(\epsilon)]^{-1}\tau_z\} + \text{H.c.}), \qquad (50)$$

where the matrix $\hat{f}$ has the standard form

$$\hat{f}(\epsilon, V) = \begin{pmatrix} \tanh\left(\dfrac{\epsilon + eV}{2T}\right) & 0 \\ 0 & \tanh\left(\dfrac{\epsilon - eV}{2T}\right) \end{pmatrix}. \qquad (51)$$

Equation (50) can be straightforwardly evaluated since the (Fourier transformed) matrices $(\hat{M}^{R,A})^{-1}$ depend now only on one energy ϵ [$\hat{g}_L$ in Eq. (39) is proportional to $\delta(\epsilon - \epsilon')$ in this case] and hence can easily be inverted analytically. Similar simplifications can also be performed in the self-consistency Eq. (41).

IV. RESULTS AND DISCUSSION

A. *SAN* junction

1. *s-wave superconductors*

We commence by calculating the differential conductance of an *SAN* contact assuming the *s*-wave pairing symmetry in a superconducting electrode. As it was already pointed out above, Eqs. (50) and (51) allow one to proceed analytically. From these equations one obtains the expression for current which consists of two parts. The first part originates from the integration over subgap energies $\epsilon < \Delta$ and yields the dominant contribution to the current at low temperatures. The other part comes from integration over energies $\epsilon > \Delta$. At low voltages and temperatures (lower than the gap Δ) this second part gives a negligible contribution to the current. Considering below the subgap contribution only, we find

$$I = \frac{e\Gamma_L\Gamma_R}{4}\int_{-\infty}^{\infty}\frac{d\epsilon}{2\pi}\mathcal{B}(\epsilon)\left[\tanh\left(\frac{\epsilon+eV}{2T}\right)-\tanh\left(\frac{\epsilon-eV}{2T}\right)\right],\tag{52}$$

where at subgap voltages and energies one has

$$\mathcal{B}(\epsilon)$$
$$=\frac{\Delta^2\theta(|\Delta|-|\epsilon|)}{\Delta^2-\epsilon^2}\frac{\Gamma_L\Gamma_R}{\left(\widetilde{\epsilon}^2+\frac{\Gamma_L^2}{4}+\frac{\Gamma_R^2}{4}\frac{\Delta^2}{\Delta^2-\epsilon^2}-\chi\right)^2+\Gamma_L^2\chi},\tag{53}$$

and

$$\chi=\left(\epsilon+\gamma_-+\frac{\Gamma_R}{2}\frac{\epsilon}{\sqrt{\Delta^2-\epsilon^2}}\right)^2.\tag{54}$$

In the limit $eV \ll \Delta$ and $T \to 0$ for the conductance $G \equiv I/V$ we obtain

$$G=\frac{e^2}{h}\frac{\Gamma_L^2\Gamma_R^2}{\left(\frac{\Gamma_L^2+\Gamma_R^2}{4}+\widetilde{\epsilon}^2-\gamma_-^2\right)^2+\gamma_-^2\frac{\Gamma_L^2}{4}}.\tag{55}$$

In order to recover the expression for G in the noninteracting limit in Eq. (55) one should simply put $\gamma_- = 0$. In a symmetric case $\Gamma_L = \Gamma_R$ and for $\widetilde{\epsilon} \to 0$ Eq. (55) reduces to the well-known result[26]
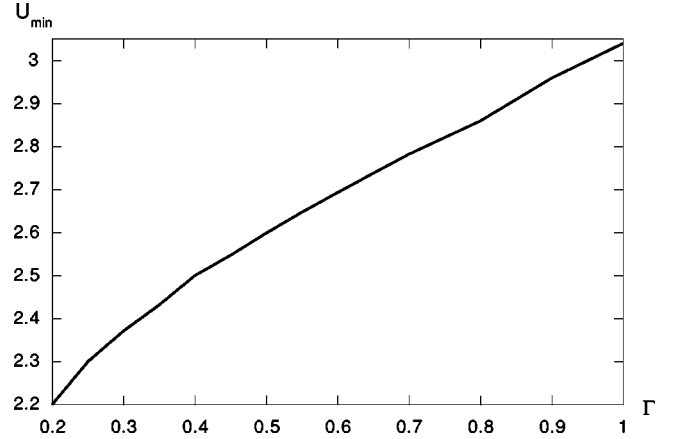

FIG. 1. The lower bound Hubbard interaction U_{min} as a function of Γ at $eV=\Delta$ for the bare level position $\epsilon_0=-1.5$ of an *SAN* junction with an *s*-wave symmetry superconductor (the parameters U, Γ, and ϵ_0 are given in units of Δ).

$$G_{NS}=2G_{NN}=\frac{4e^2}{h}.\tag{56}$$

In the presence of Coulomb interaction the parameter γ_- in Eqs. (53)–(55) should be determined from the self-consistency Eq. (41). It has a physical meaning as an energy proportional to the difference pertaining to spin-up and spin-down populations of electrons on the level. We are looking for solution of Eq. (41) which gives nonzero value of this parameter. In the introduction we noticed that the solution exists if $U > -\epsilon_0$. The presence of nonzero bias V as well as interaction itself modifies this condition and put a restriction on the lower bound of U for which there is a solution of Eq. (41). Generally, at a given Γ this lower bound for interaction U_{min} increases when the voltage grows, more strongly for *SAN* junction and less for *SAS* ones. The same is true if we increase the transparency Γ. Figure 1 displays such a dependence of U_{min} as function of Γ at $eV=\Delta$.

The parameter U_{min} plays the important role of being a lower bound on the Hubbard energy U for which the single occupancy solution of mean-field Eq. (41) (doublet state) still exists. The other state (a singlet), which is relevant for the Kondo limit[11,12] cannot be obtained in the MF approximation. It turn out to be important for higher values of U and when the Kondo temperature $T_K=\sqrt{U\Gamma}\exp[-\pi|\epsilon_0|/2\Gamma]$ is larger than Δ. In the present study we do not consider the Kondo limit,[10–12] assuming that T_K is small and thus the single occupancy solution represents the ground state of the system.

The calculation of the tunneling current then proceed as Eq. (41) is solved numerically for a given set of system parameters. To be definite, the parameters $\Gamma_L=\Gamma_R=\Gamma=0.35\Delta$ are adopted, and the more interesting subgap voltage bias regime $eV\lesssim 2\Delta$ is considered in the low-temperature limit $T\to 0$. The values of the Hubbard repulsion parameter U were fixed to be $U=2.450\Delta$ and $U=2.713\Delta$. As a reference we also consider a noninteracting localized state[3] in the off-resonance case that formally corresponds to the limit $U=\gamma_-=0$, although, as we noticed above, this
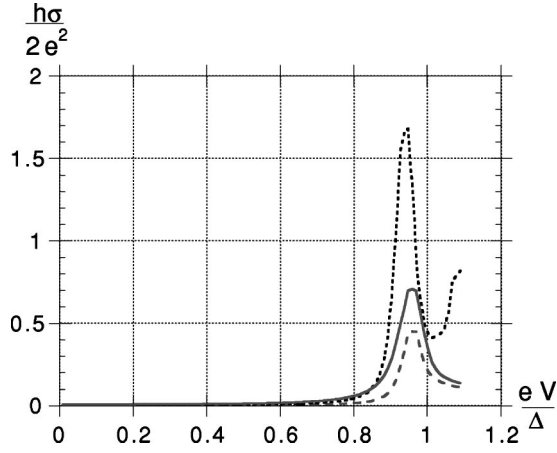
FIG. 2. Differential conductance of an *SAN* junction with an *s*-wave symmetry superconductor. The figure displays the dependence of Andreev conductance on the applied voltage for $U = 2.450$ (dot curve) and $U = 2.713$ (dashed curve) and $U = \gamma_- = 0$ (solid curve). The barrier transparency is $\Gamma = 0.35$ and the dot level energy is $\epsilon_0 = -1.5$ (the parameters U, Γ, and ϵ_0 are given in units of Δ).

limit cannot be reached by a gradually decreasing U. For convenience all energy parameters are scaled, namely, ϵ, U, $\Gamma_{L,R}$, and T are expressed in units of Δ. The current and the conductance are respectively expressed in units of $\Delta e/\hbar$ and $e^2/2h$.

The dependence of γ_- on the bias V has a considerable impact on the differential conductance $\sigma = dI/dV$ which we calculate numerically. The corresponding results are presented in Fig. 2. It is readily seen that for a given set of parameters the conductance virtually vanishes in a substantial part of the subgap region. Note, however, that at voltages close to but still smaller than Δ/e the differential conductance σ increases sharply. This feature can be understood as a result of interplay between Coulomb blockade and two electron tunneling effects. It is well known[26] that the subgap conductance in *SN* junctions is caused by the mechanism of Andreev reflection during which the charge $2e$ is transferred between the electrodes. Without interaction Eq. (55) with $U = \gamma_- = 0$ holds at $V \to 0$. The conductance versus voltage dependence in the whole subgap region is represented in this case ($U = \gamma_- = 0$) by the solid curve in Fig. 2. Unlike the resonance limit Eq. (56), which corresponds to perfect transparency of the channel here we clearly see a maximum near the gap region. This effect is related to the small transparency of the junction due to the off-resonance condition, when increasing the BCS density of states at the gap is im-

portant (a shift from Δ in the position of the peak originates from a small inelastic term we added to the energy). In the presence of interaction, at $T = 0$, the nonzero solution γ_- of the self-consistent Eq. (41) appears. It represents the Coulomb blockade influence on electron tunneling which acts in the mean-field approximation by changing the position of the level and also, through the value of γ_-, by changing the energy of spin-up and spin-down electrons. In the strongly interacting regime the single occupancy energy γ_- is not zero even if the renormalized level position $\tilde{\epsilon}$ vanishes. This drives the conductance to small values of V Eq. (55) and turns the current behavior to be like that corresponding to tunneling through a localized level out of resonance. The height of the maximum and the exact voltage at which the current is ''turned on'' are in the vicinity to the gap as in Fig. 2 for all $0.3 < \Gamma \leqslant 1$. Although the above height and voltage are affected by interaction, the presence of the gap is manifested.

It is interesting to point out that the highest peak in the conductance near the superconducting gap is obtained when the Hubbard energy U approaches the value U_{min}. As was noticed earlier, U_{min} is the low boundary value of the interaction at which the MF approximation is valid for voltage $eV = \Delta$. For $U < U_{min}$ there is no solution of Eq. (41) for the single occupancy parameter γ_-.

There exists a certain analogy between our results and those obtained for superconductor-ferromagnet (*SF*) junctions.[27] Here the repulsion parameter U plays a role similar to that of an exchange term in *SF* systems: in both cases the subgap conductance can be tuned by changing this parameter in a way that a smaller value of U corresponds to a weaker exchange field. In contrast to the case under study here, however, changing of the exchange field in *SF* junctions leads to smooth variations of the subgap conductance.[27]

Let us now briefly consider the limit of large bias voltages $eV \gg \Delta$. In this case the current may be represented as a sum of two terms $I = I_1 + I_2$. The term I_1 is determined by an expression similar to Eq. (52) which now includes the contribution from energies above the gap. We find

$$I_1 = \frac{e\Gamma_L \Gamma_R}{4} \int_{-\infty}^{\infty} \frac{d\epsilon}{2\pi} [\mathcal{B}(\epsilon) + \mathcal{B}_1(\epsilon)]$$

$$\times \left[\tanh\left(\frac{\epsilon + eV}{2T}\right) - \tanh\left(\frac{\epsilon - eV}{2T}\right) \right]. \qquad (57)$$

Here $\mathcal{B}(\epsilon)$ is again given by Eq. (53) while the function $\mathcal{B}_1(\epsilon)$ reads

$$\mathcal{B}_1(\epsilon) = \frac{2|\epsilon| \theta(|\epsilon| - |\Delta|)}{\epsilon^2 - \Delta^2} \frac{[\tilde{\epsilon}^2 + (\epsilon + \gamma_-)^2 + \chi_1]}{[\tilde{\epsilon}^2 - (\epsilon + \gamma_-)^2 + \chi_1]^2 + (\epsilon + \gamma_-)^2 \left(\Gamma_L + \Gamma_R \frac{|\epsilon|}{\sqrt{\epsilon^2 - \Delta^2}} \right)^2}. \qquad (58)$$

We also define

$$\chi_1 = \frac{1}{4}\left(\Gamma_L^2 + \Gamma_R^2 + 2\Gamma_L\Gamma_R\frac{|\epsilon|}{\sqrt{\epsilon^2-\Delta^2}}\right). \qquad (59)$$

The other contribution I_2 is proportional to the level position $\widetilde{\epsilon}$. One obtains

$$I_2 = \frac{e\Gamma_L\Gamma_R}{4}\int_{-\infty}^{\infty}\frac{d\epsilon}{2\pi}\mathcal{B}_2(\epsilon)\left[\tanh\left(\frac{\epsilon+eV}{2T}\right)\right.$$

$$\left. +\tanh\left(\frac{\epsilon-eV}{2T}\right)-2\tanh\left(\frac{\epsilon}{2T}\right)\right]. \qquad (60)$$

The expression for $\mathcal{B}_2(\epsilon)$ can be obtained from Eq. (58) if one replaces the term in the square brackets by the expression $-2\widetilde{\epsilon}(\epsilon+\gamma_-)$.

The above results together with the self-consistency equation for γ_- provide a complete description for the I-V curve of an *SAN* junction in the presence of interactions. In all interesting limits the energy integrals in Eqs. (57) and (60) can be carried out and the corresponding expressions for the current can be obtained. These general expressions, however, turn out to be quite complicated and will not be analyzed in detail further below. Here we just demonstrate that in the noninteracting limit $\gamma_-=0$ our results reduce to those already familiar in the literature. Indeed, in the leading order approximation, Eqs. (57) and (58) yield the standard Breit-Wigner formula

$$\sigma = \frac{2e^2}{h}\frac{\Gamma_L\Gamma_R}{\dfrac{(\Gamma_L+\Gamma_R)^2}{4}+\widetilde{\epsilon}^2}. \qquad (61)$$

After setting $\widetilde{\epsilon}=0$ and $\Gamma\gg\Delta$ in Eqs. (57), (53), and (58) in the limit $eV\gg\Delta$ one easily obtains the contributions to the current equal to $2G_{NN}\Delta/e$ and $G_{NN}(V-2\Delta/3e)$, respectively, from the subgap energies ($\mathcal{B}$) and from energies above the gap ($\mathcal{B}_1$). The sum of these contributions yields the standard result

$$I = G_{NN}(V+4\Delta/3e). \qquad (62)$$

The second term represents the so-called excess current which originates from the mechanism of Andreev reflection. It follows from our general analysis that in quantum dots this current is also affected by Coulomb interaction.

2. Superconductors with unconventional pairing

Since the order parameter Δ for p- and d-wave superconductors is not isotropic, the magnitude of the current is sensitive to the junction geometry. As discussed before, here we consider a system of two planar superconducting (or normal) strips with electron tunneling between them along the x axis through the dot located at $x=y=0$. For d-wave superconductors we choose the nodal line of the pair potential on the Fermi surface to coincide with the tunneling direction (Fig. 3), such that $\Delta=v_\Delta p_{P_F}\sin 2\alpha$. The direction of tunneling corresponds to the angle $\alpha=0$. For spin-triplet supercon-
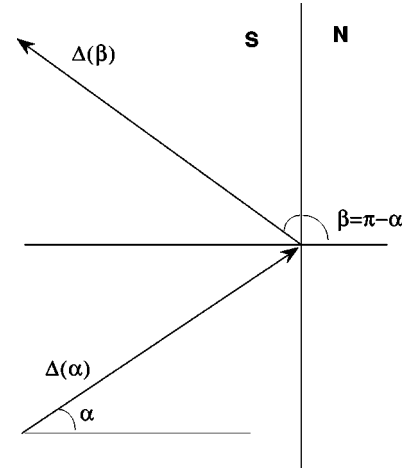

FIG. 3. Schematic geometry of the junction. The left half plane is a superconductor and the right one is a normal metal. Incoming and reflected electronlike excitations are moving in an angle-dependent pair potential which can have different signs for these quasiparticles.

ducting states the order parameter is an odd vector function of momentum and a 2×2 matrix in spin space. We choose to represent it by a time-reversal symmetry-breaking state[14] which is off-diagonal in spin indices. In the geometry of Fig. 3, α is the azimuthal angle in the x-y plane and the order parameter can approximately be represented as $\Delta=\Delta_0\exp(i\alpha)$. This order parameter can possibly describe pairing in a superconductor Sr_2RuO_4 which was recently discovered.[13] The pair potential so chosen within the geometry of the junction may have different signs for incoming and reflected quasiparticles moving at the angles α and $\pi-\alpha$, respectively. This fact significantly affects the scattering process[15] and causes the formation of a zero energy (midgap) bound state[17] centered at the boundary. For this state we calculate the Green function $\hat{G}$ which, like in the case of s-wave superconductors, satisfies Eq. (16) with a δ function on the right side and require $\hat{G}$ to vanish at $x=0$. The distinction of solutions for d- or p-wave superconductors from those found above for the s-wave case is due to the sign change of the pair potential: reflected quasiparticles propagate in a pair potential of an opposite sign compared with Δ as "seen" by incoming quasiparticles. The equilibrium retarded and advanced Eilenberger-Keldysh functions $\hat{g}^{R,A}$ for p-wave superconductors read

$$\hat{g}^{R,A}(\epsilon) = \frac{\sqrt{(\epsilon\pm i0)^2-\Delta^2}-\tau_+\Delta+\tau_-\Delta^*}{\epsilon\pm i0}. \qquad (63)$$

The I-V curve for an *SAN* junction with electrodes composed of p-wave superconductors and *with Hubbard interaction* is remarkably distinct from those found for the s-wave case (cf. Figs. 2 and 4). This difference is predominantly due to the surface bound state which exists in the p-wave case and causes the conductance peak in the subgap region. Due to electron-electron repulsion this peak is split and appears at
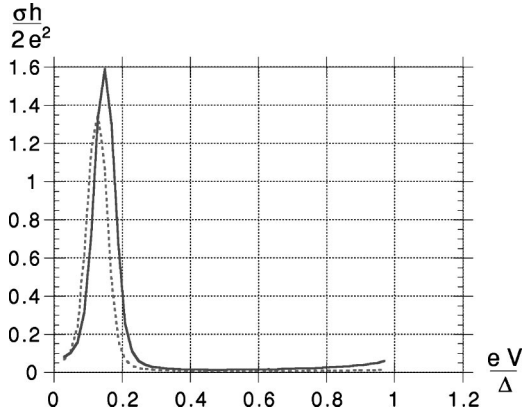
FIG. 4. Same as in Fig. 2 but for a p-wave symmetry superconductor. The figure displays the dependence of Andreev conductance on the applied voltage for $U=2.4$ (solid curve) and $U=2.713$ (dot curve). The barrier transparency is $\Gamma=0.35$ and the dot level energy is $\epsilon_0=-1.5$

$V\neq 0$, see Fig. 4. Here again, the repulsion attenuates the conductance, which is larger for $U=2.45\Delta$ than for $U=2.713\Delta$.

B. *SAS* junction

We focus first on the noninteracting case $U=0$ and briefly consider pure resonant tunneling at the Fermi level, i.e., set $\epsilon_0\to 0$. This situation corresponds to a ballistic *SNS* junction with only one conducting channel. Current-voltage characteristics of ballistic *SNS* junctions were intensively studied in the past.[2,28–33] If the relevant energies are small as compared to Γ (for short junctions this condition usually means $\Gamma>\Delta$), S_{dot} in Eq. (26) can be dropped and one gets $\langle \bar{c}c\rangle=\hat{g}_+^{-1}\tau_z/\Gamma$. Equation (32) then yields

$$I=\frac{e}{2}\text{Tr}\tau_z\hat{g}_-\hat{g}_+^{-1}|_K. \tag{64}$$

Note that here the tunneling rate Γ just cancels out. In the many channel limit Eq. (64) coincides with the quasiclassical result.[28,29] For a constant bias V the matrix $\hat{g}_+^{-1}$ can be evaluated analytically,[30] yielding the I-V curve of a ballistic *SNS* junction. In particular, in the zero-bias limit $V\to 0$ and for $\Gamma\gg\Delta$ one recovers the MAR current:[30]

$$I_{AR}=\frac{2e^2}{h}\frac{2\Delta}{eV}V=\frac{4e\Delta}{h}. \tag{65}$$

The corresponding explicit calculation performed within our formalism is presented in the Appendix.

Now we consider *SAS* junctions with Hubbard interaction included.

1. s-wave superconductors

In order to calculate the subgap current in the case of an *SAS* junction with Coulomb interaction one has first to find the solution of the self-consistency Eqs. (48). This requires the inversion of the matrix $\hat{M}$ in energy and spin spaces. If
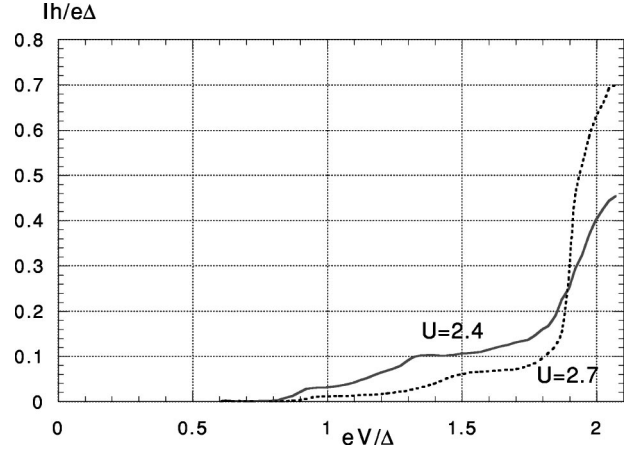

FIG. 5. The subgap tunneling current in units $2e\Delta/h$ versus voltage for an *SAS* junction with s-wave symmetry superconductors. The parameters (in units of Δ) are $U=2.4$ (solid curve), $U=2.7$ (dot curve), $\epsilon=-1.5$, and $\Gamma=0.6$.

the number of modes for each energy in the interval $[0,2eV]$ is cut off at some integer m, the size of the pertinent matrices is $(4m+2)\times(4m+2)$. The number m of energy slices has to be adjusted in such a way that the results become insensitive to it. This requires larger m for smaller voltages because quasiparticles can escape the gap region after undergoing a large number of Andreev reflections.

In the MF approximation which is used to analyze the Hubbard interaction, the Anderson level is effectively reduced to a free level out of resonance, which interacts only with the superconductors. The Coulomb repulsion is the cause of nonzero single occupancy energy γ_-. This energy is included in the deviation of the free level from resonance. Thus tunneling through an Anderson impurity center is represented by tunneling through an energy level out of resonance. The farther is the level from resonance, the weaker is the effective transparency of the junction. In an *SAS* junction, the main process contributing to the subgap current is multiple Andreev reflections (MAR). However, in spite of the fact that for low V the number $n\approx 2\Delta/eV$ of MAR is large, the current density is rather weak. This is due to the low effective transparency of the junction as a consequence of interaction (Coulomb blockade). Indeed, in *SAS* junctions, the interaction produces an effective transparency which is of the same order as in Eq. (56) for an *SAN* contact. If the transparency of the junction is less than unity, then every next Andreev reflection is suppressed by the power of the effective transparency. This is due to the fact that the current depends in a nonlinear way on the tunneling amplitude, and Andreev reflection is combined with ordinary scattering at the *SA* interface. Therefore the high-n processes are of higher order in the tunneling strength and will be suppressed as the nth power of the effective transparency. Thus there is a strong suppression of the current at low voltages when the number of Andreev reflections is large. This is what is observed in our Fig. 5.

The I-V characteristics for tunneling between two s-wave superconductors is displayed in Fig. 5. The transparency of the junction is chosen to be $\Gamma=0.6\Delta$ and the current is
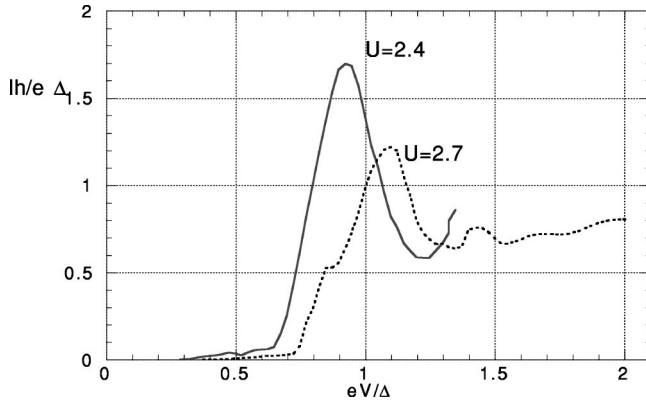
FIG. 6. Same as Fig. 4 but for p-wave symmetry superconductors.

evaluated for $U=2.4\Delta$ and $U=2.7\Delta$. One notices that at relatively low bias voltages $eV\lesssim0.8\Delta$ for $U=2.4\Delta$ and $eV\lesssim(0.9-0.95)\Delta$ for $U=2.7\Delta$ the subgap current is essentially suppressed. For higher voltages the subgap current increases rather sharply, as a result of an interplay between Coulomb blockade and multiple Andreev reflections. The latter mechanism manifests itself in the occurrence of subharmonic peaks in the differential conductance. Due to interaction, the subgap current as we note above is strongly depressed at low voltages. The positions of peaks in the conductance are shifted relative to those in the noninteracting case $eV=2\Delta/n$, where n is the number of Andreev reflections and are as can be seen in Fig. 5, increasing U results in a larger shift of peak positions.

In the limit of high voltages $eV\gg\Delta$ the I-V curves for SAS junctions are analogous to those for SAN ones except the excess current is two times larger.

2. Superconductors with unconventional pairing

Similarly to the case of SAN junctions, there is an important difference in the tunneling current between SAS junctions with interaction depending on whether the order parameter in the electrodes is of s- or p-wave symmetry. The I-V curve for the latter case is depicted in Fig. 6. We observe that the subgap current for p-wave superconductors is considerably larger than for s-wave ones, roughly by $I_{max}^{(p)}/I_{max}^{(s)}\approx8$. On the other hand, the effect of the Coulomb repulsion U at low voltages is rather similar: there is a strong suppression of the subgap current because high-n MAR processes are damped by the n power of transparency which is small due to Coulomb repulsion. For $U=2.7\Delta$ the current is suppressed compared to its value at $U=2.4\Delta$. Beside the distinction of magnitudes, there is an unusual additional structure in the I-V curves for p-wave superconductors which is related to the presence of a surface bound state. Comparing the results presented in Figs. 5 and 6 we observe that in the latter case, the current peaks at a certain bias voltage. This implies a negative differential conductance, which is the hallmark of resonant tunneling (contributed by the bound state).

Our analysis of the junctions formed by p-wave superconductors can be straightforwardly extended to the case of d-wave pairing. The I-V curves and the subharmonic gap

structure in junctions with d-wave superconductors in the absence of Coulomb interaction was recently studied (see, e.g., Ref. 34 and other references therein). Near zero bias the I-V curves[34] exhibit a current peak (equivalently, negative differential conductance) related to the presence of midgap surface states. Notice that in such systems the symmetry restricts the current, so that the contribution from the bound midgap states may vanish if, for instance, one assumes $\mathcal{T}_{L,R}^2$ to be independent of v_x. As we have already argued before (see also Ref. 24), it might be essential to take the dependence of tunneling matrix elements on v_x into account already for point contacts. One can also consider the impurity model different from a pointlike defect. Such a situation can be realized, e.g., by artificially induced defects.[35] The spectroscopy of $Bi_2Sr_2CaCu_2O_8$ surfaces indicates that such defects appear to be more extended in scanning tunnel microscope imaging. In this case one can expect nonzero contribution from midgap level also in d-waves superconductors. Here, again, the electron-electron repulsion shifts the peak positions from their ''noninteracting'' values $eV=2\Delta/n$ to higher voltages. It is quite likely that this interaction-induced shift was observed in the experiment.[36]

V. CONCLUSIONS

In this paper the tunneling between two superconductors or between a superconductor and normal metal through an Anderson-type quantum dot is investigated. Special attention is devoted to analyze the implications of the Coulomb repulsion between electrons in the dot on the tunneling process. The Andreev conductance for an SAN junction and the subgap current in an SAS junction are calculated and elaborated upon. The theoretical treatment requires a combination of the Keldysh nonequilibrium Green function and path integral formalism and the dynamical mean-field approximation. We derive general expressions for the effective action and the transport current through the system. These expressions are then employed in order to obtain a workable formula for the current. The latter is then calculated analytically and numerically for a certain set of energy parameters.

The main results of the present research can be summarized as follows: (i) When one of the electrodes is a normal metal (an SAN junction) the gap symmetry structure is exhibited in the Andreev conductance. For p-wave superconductors, it shows a remarkable peak for voltages in the subgap region. For s-wave superconductors, on the other hand, the position of the peak is shifted towards the gap edge. It is further demonstrated that the highest peak in the conductance is reached if the Hubbard repulsive interaction approaches U_{min}. Recall that at this value of $U=U_{min}$ the MF approximation is not valid anymore and the single occupancy solution ceases to exist. (ii) The dynamics of tunneling between two superconductors (an SAS junction) is more complicated. For s-wave superconductors the usual peaks in the conductance that originate from multiple Andreev reflections[2] are shifted by interaction to higher values of V. The subgap current suffers sizable suppression at low voltages though the number of Andreev reflections is large. This is because the high-n order MAR are suppressed by n power

of effective transparency of the junction. This effective transparency mainly is defined by Hubbard interaction and becomes smaller when Hubbard interaction strength increases. The subgap current in this case may describe the low energy channels in break junctions.[6] For p-wave superconductors, the subgap current is much larger than in the s-wave case and the I-V characteristics exhibits an interesting feature: the occurrence of midgap bound state results in a peak in the current, that is, a negative differential conductance.

APPENDIX

Below we will derive the result (65) within the framework of the formalism developed in the present paper. Consider a quantum dot between two s-wave superconductors and assume that the interaction is negligibly small $U \to 0$. For the sake of simplicity we will also set $\Gamma_L = \Gamma_R = \Gamma$. The result (42) can be expressed as a sum of two terms $I = I_{AR} + I_{qp}$, where

$$I_{AR} = -\frac{e\Gamma^2}{4h} \int_0^{2eV} d\epsilon \, \mathrm{Tr}[(\tilde{N}_R)^{12}(\tilde{g}_L^A)^{21} - (\tilde{N}_L)^{12}(\tilde{g}_R^A)^{21}$$
$$- (\tilde{N}_R)^{21}(\tilde{g}_L^R)^{12} + (\tilde{N}_L)^{21}(\tilde{g}_R^R)^{12}], \quad \text{(A1)}$$

$$I_{qp} = -\frac{e\Gamma^2}{4h} \int_0^{2eV} d\epsilon \, \mathrm{Tr}[(\tilde{N}_R)^{11}((\tilde{g}_L^A - g_L)^R)^{11}$$
$$- (\tilde{N}_L)^{11}((\tilde{g}_R^A - \tilde{g}_R)^R)^{11}]. \quad \text{(A2)}$$

Here I_{AR} is the subgap (Andreev reflection) contribution to the averaged current while I_{qp} is defined by the excitations above the gap. In Eqs. (A1) and (A2) we defined the Green-Keldysh matrices $\tilde{g} = i\tau_z \hat{g}$ with

$$\tilde{g}_{R,L}^{R,A}(\epsilon) = F^{R,A}(\epsilon)(\epsilon + \tau_+ \Delta + \tau_- \Delta^*), \quad \text{(A3)}$$

$$F^{R,A}(\epsilon) = \frac{\theta(|\Delta| - |\epsilon|)}{\sqrt{\Delta^2 - \epsilon^2}} \pm i \, \mathrm{sgn}(\epsilon) \frac{\theta(|\epsilon| - |\Delta|)}{\sqrt{\epsilon^2 - \Delta^2}}, \quad \text{(A4)}$$

$$\tilde{g}_{R,L}^K(\epsilon) = [\tilde{g}_{R,L}^R(\epsilon) - \tilde{g}_{R,L}^A(\epsilon)]\tanh(\epsilon/2T). \quad \text{(A5)}$$

We also defined

$$\tilde{N}_{L,R}^{ij} = (\tilde{M}^R \tilde{g}_{L,R}^K \tilde{M}^A)^{i,j}, \quad \tilde{M}^{R,A} \equiv (M^{R,A})^{-1}, \quad \text{(A6)}$$

where the superscripts stand for the spin indices in Nambu space and Tr denotes the remaining trace over (discrete) energies which are scaled to Δ throughout this Appendix.

Consider the limit of small voltages $eV \ll \Delta$. In this limit the subgap current I_{AR} can be rewritten in the form

$$I_{AR} = -\frac{e^2V}{h} \sum_{m,n} [\tilde{g}^K(E_m)([m|(\tilde{M}^A)^{i2}|n]$$

$$\times [n+1|(\tilde{M}^R)^{1i}|m]F^A(E_n^+) - [m|(\tilde{M}^A)^{i1}|n]$$

$$\times [n-1|(\tilde{M}^R)^{2i}|m]F^R(E_n^-)) - \tilde{g}^K(E_m^-)([m|(\tilde{M}_A)^{12}|n]$$

$$\times [n|(\tilde{M}^R)^{11}|m]F^A(E_n) - [m|(\tilde{M}^A)^{11}|n]$$

$$\times [n|(\tilde{M}^R)^{21}|m]F^R(E_n)) - \tilde{g}^K(E_m^+)([m|(\tilde{M}^A)^{22}|n]$$

$$\times [n|(\tilde{M}^R)^{12}|m]F^A(E_n) - [m|(\tilde{M}^A)^{21}|n]$$

$$\times [n|(\tilde{M}^R)^{22}|m]F^R(E_n))]. \quad \text{(A7)}$$

Here we denote $E_n^{\pm} = eV(2n \pm 1)$ and $E_n = 2eVn$. We also included $\Gamma/2$ into the definition of $\tilde{M}$ and omitted terms nondiagonal in the spin indices because these terms are small in the limit $eV \ll \Delta$. At $T \to 0$ the summation over m is reduced to just one term with the maximum number m_0 determined by the condition: $|E_{m_0}| = 1$.

It is straightforward to evaluate the matrices $(m_0|\tilde{M}^{i,j}|n)$ for sufficiently large $\Gamma > \Delta$ and $\epsilon_0 \to 0$. In this case $\tilde{M}^{i,j}$ satisfy the following approximate equations:

$$[m|(\tilde{M}^R)^{11}|m_0](E_m^2/4 - 2)$$
$$= -E_m \delta_{m,m_0}/2F^R(E_m) + [m-1|(\tilde{M}^R)^{11}|m_0]$$
$$+ [m+1|(\tilde{M}^R)^{11}|m_0], \quad \text{(A8)}$$

$$[m|(\tilde{M}^R)^{12}|m_0] = -4[m|(\bar{M}^R)^{12}|m_0]$$
$$\times [E_m F^R(E_m) E_{m_0}^- F^R(E_{m_0}^0)^{-1}], \text{(A9)}$$

$$[m|(\bar{M}^R)^{12}|m_0](E_m^2/4 - 2)$$
$$= [\delta_{m,m_0} + \delta_{m-1,m_0}]E_m^2 F^R(E_m)/4$$
$$+ [m-1|(\bar{M}_R)^{12}|m_0] + [m+1|(\bar{M}_R)^{12}|m_0]. \quad \text{(A10)}$$

Similar equations can easily be derived for the two remaining blocks. In the leading order in m_0 (this approximation is justified at small voltages $V \to 0$) at subgap energies ($E_n < 1, F^R = F^A = F$) we obtain

$$[n|(\tilde{M}^R)^{11}|m_0] = \frac{(-1)^n(n+1)}{(m_0+2)F(E_{m_0}^-)}, \quad \text{(A11)}$$

$$[n|(\tilde{M}^R)^{12}|m_0] = \frac{(-1)^n(n+1)E_{m_0}}{(m_0+2)E_n F(E_n)}, \quad \text{(A12)}$$

$$[n|(\tilde{M}^R)^{21}|m_0] = -\frac{(-1)^n(n+1)E_{m_0}}{(m_0+2)E_n F(E_n)}. \quad \text{(A13)}$$

Substituting these matrix elements into Eq. (A7) and performing a simple summation over n we arrive at the result (65).

*Email address: yshai@bgumail.bgu.ac.il

[1] T.M. Klapwijk, G.E. Blonder, and M. Tinkham, Physica B & C **109+110B**, 1157 (1982).

[2] G.B. Arnold, J. Low Temp. Phys. **59**, 143 (1985).

[3] A. Golub, Phys. Rev. B **52**, 7458 (1995).

[4] L.I. Glazman and K.A. Matveev, Zh. Éksp. Teor. Fiz. Pis'ma Red. **49**, 570 (1989) [JETP Lett. **49**, 659 (1989)].

[5] D.C. Ralph, C.T. Black, and M. Tinkham, Phys. Rev. Lett. **74**, 3241 (1995).

[6] E. Scheer *et al.*, Phys. Rev. Lett. **78**, 3535 (1997); J.M. van Ruitenbeek, cond-mat/9910394 (unpublished).

[7] J.C. Cuevas, A. Levy Yeyati, and A. Martin-Rodero, Phys. Rev. Lett. **80**, 1066 (1998).

[8] S.M. Cronenwett, T.H. Oosterkamp, and L.P. Kouwenhoven, Science **281**, 540 (1998).

[9] D. Goldhaber-Gordon, J. Gores, M.A. Kastner, H. Shtrikman, D. Mahalu, and U. Meirav, Phys. Rev. Lett. **81**, 5225 (1998).

[10] A. Golub, Phys. Rev. B **54**, 3640 (1996).

[11] R. Fazio and R. Raimondi, Phys. Rev. Lett. **80**, 2913 (1998); **82**, 4950(E) (1999).

[12] A.A. Clerk, V. Ambegoakar, and S. Hershfield, Phys. Rev. B **61**, 3555 (2000).

[13] Y. Maeno *et al.*, Nature (London) **372**, 532 (1994).

[14] T.M. Rice and M. Sigrist, J. Phys.: Condens. Matter **7**, 643 (1995).

[15] T. Hirai, K. Kusakabe, Y. Tanaka, Physica C **336**, 107 (2000).

[16] L. Buchholtz and G. Zwicknagl, Phys. Rev. B **23**, 5788 (1981).

[17] C.-R. Hu, Phys. Rev. Lett. **72**, 1526 (1994).

[18] A.V. Rozhkov and D.P. Arovas, Phys. Rev. Lett. **82**, 2788 (1999).

[19] Y. Avishai and A. Golub cond-mat/9909098, Phys. Rev. B (to be published).

[20] L.V. Keldysh, Zh. Éksp. Teor. Fiz. **47**, 1515 (1964) [Sov. Phys. JETP **20**, 1018 (1965)].

[21] G. Schön and A.D. Zaikin, Phys. Rep. **198**, 237 (1990).

[22] R.P. Feynman and F.L. Vernon, Jr., Ann. Phys. (N.Y.) **24**, 118 (1963); R. P. Feynman and A. R. Hibbs, *Quantum Mechanics and Path Integrals* (McGraw Hill, New York, 1965).

[23] G. Eilenberger, Z. Phys. **214**, 195 (1968); A.I. Larkin and Yu.N. Ovchinnikov, Zh. Éksp. Theor. Phys. **68**, 1915 (1975) [Sov. Phys. JETP **41**, 960 (1975)]; For a recent review, see also W. Belzig, F.K. Wilhelm, C. Bruder, G. Schön, and A.D. Zaikin, Superlattices Microstruct. **25**, 1251 (1999).

[24] Yu.S. Barash, A.V. Galaktionov, and A.D. Zaikin, Phys. Rev. B **52**, 665 (1995); Phys. Rev. Lett. **75**, 1675 (1995).

[25] A.T. Alastalo and M.M. Salomaa (unpublished).

[26] G.E. Blonder, M. Tinkham, and T.M. Klapwijk, Phys. Rev. B **25**, 4515 (1982).

[27] M.J.M. de Jong and C.W.J. Beenakker, Phys. Rev. Lett. **74**, 1657 (1995).

[28] A.V. Zaitsev, Zh. Eskp. Teor. Fiz. **78**, 221 (1980) [Sov. Phys. JETP **51**, 111 (1980)].

[29] A.D. Zaikin, Zh. Eskp. Teor. Fiz. **84**, 1560 (1983) [Sov. Phys. JETP **57**, 910 (1983)].

[30] U. Gunsenheimer and A.D. Zaikin, Phys. Rev. B **50**, 6317 (1994).

[31] D.V. Averin and D. Bardas, Phys. Rev. Lett. **75**, 1831 (1995).

[32] E.N. Bratus, V.S. Shumeiko, and G. Wendin, Phys. Rev. Lett. **74**, 2110 (1995).

[33] J.C. Cuevas, A. Martin-Rodero, and A. Levy Yeyati, Phys. Rev. B **54**, 7366 (1996).

[34] T. Löfwander, G. Johansson, and G. Wendin, cond-mat/9908261 (unpublished).

[35] A. Yazdani *et al.*, Phys. Rev. Lett. **83**, 176 (1999).

[36] A. Engelhardt, R. Dittmann, and A.I. Braginski, Phys. Rev. B **59**, 3815 (1999).